

# A model of TEC perturbations possibly related to seismic activity

Valery M. Sorokin<sup>1</sup>, Victor A. Novikov<sup>\*,2,3</sup>

<sup>(1)</sup> Pushkov Institute of Terrestrial Magnetism, Ionosphere, and Radio Wave Propagation, Russian Academy of Sciences, Moscow, Russia

<sup>(2)</sup> Joint Institute for High Temperatures, Russian Academy of Sciences, Moscow, Russia

<sup>(3)</sup> Sadovsky Institute of Geosphere Dynamics, Russian Academy of Sciences, Moscow, Russia

Article history: received June 1, 2023; accepted October 29, 2023

## Abstract

For application of observed anomalies of the total electron content (TEC) in the ionosphere for short-term earthquake prediction, it is necessary to understand the physical nature of such anomalies during the preparation of a strong seismic event. The physical mechanism of occurrence of such anomalies is considered in order to distinguish the TEC disturbance of a seismic origin and to clear the processes in the lithosphere resulted in an appearance of the TEC anomaly in the ionosphere. It is supposed that the observed TEC anomalies arise as a result of occurrence of additional electric field in the ionosphere demonstrated by numerous satellite data before the impending earthquakes. At the same time, an injection of charged aerosols into the atmosphere in the epicentral earthquake area was detected. As a result, an electromotive force arises in the surface layer of the atmosphere, which initiates a perturbation of the electric current in the global circuit and the electric field appearance in the ionosphere. We have shown that the TEC disturbance arises as a result of the heating of the ionosphere by electric current and the plasma drift in the electric field of this current. The spatial distribution of TEC arises as a result of the combined action of these two factors, and its nature depends on the relationship between them. Based on the developed model the numerical study of the spatial distribution of TEC in the ionosphere is possible for a given horizontal distribution of the concentration of charged aerosols in the atmosphere near the Earth's surface.

Keywords: Total electron content; Electric field; Ionosphere heating; Plasma drift; Earthquake preparation area; Charged aerosol injection

---

## 1. Introduction

Recently, the method of measuring the total electron content (TEC) of the ionosphere using GPS receivers has received the great development [Liu et al., 1996; 2004]. Research is underway to analyze the spatial distribution of TEC anomalies before earthquakes (e.g. [Astafieva, 2019], [Afraimovich et al., 2004], and references therein). In the paper [Zolotov et al., 2008] numerical modeling of the ionospheric disturbance was carried out, where the spatial distribution of TEC obtained from GPS receivers in the seismic region has been analyzed. The authors used a global model of the

upper atmosphere, which describes the thermosphere, ionosphere, and plasmasphere as a unified system. The model is based on the integration of non-stationary three-dimensional equations of continuity, momentum, and energy balance of a multicomponent gas together with the equations of electric field potential. This model has been used to calculate the additional electric field, which should result in the observed TEC anomaly. The time period before the earthquake in Peru on September 26, 2005,  $M = 7.0$  has been analyzed. The main characteristics of the TEC disturbance that appeared during six days before the earthquake from September 21 to September 26, 2005, are presented in [Zakharenkova et al., 2008]. As a result of a numerical study with the selection of an electric field of various configurations and amplitudes, it was shown in [Zolotov et al., 2008] that the observed TEC disturbance is possible with an additional electric field of 6 mV/m. It is assumed in [Klimenko et al., 2011; 2012; Namgaladze et al., 2009] that the possible main cause of the TEC disturbance is the vertical plasma drift due to the action of the zonal electric field. Numerical modeling performed in [Klimenko et al., 2012] showed that the amplitude of this electric field should be 3 to 9 mV/m.

The most informative data on TEC anomalies of seismic nature were obtained during the earthquake with  $M = 8.0$ , which occurred on May 12, 2008 at 06:28 UT in Sichuan province in China. The data were provided by the dense network of GPS receivers and ionosondes in China. Images were obtained on the maps of the TEC anomaly distribution with detailed spatial and temporal resolution (1 hour). The sequence of images shows a detailed development of a positive TEC anomaly southeast of the earthquake epicenter [Zhao et al., 2010]. The anomaly develops after 15:00 LT and reaches its maximum between 18:00 and 19:00 LT. A similar image of this anomaly was also obtained by other authors [Klimenko et al., 2011]. The maps show a weak and less pronounced anomaly in the southern hemisphere. Observations showed a 100% anomalous TEC increase compared with the 15-day average value in the afternoon of May 9, 2008. At the same time, the geomagnetic situation was quiet ( $K_p \leq 2$ ). It was shown that the area of predominant TEC increase was localized in the interval of longitudes  $90^\circ - 130^\circ\text{E}$ . Based on the obtained results, the authors supposed that the anomalous TEC increase was most likely due to the preparation of an earthquake with the epicenter coordinates  $30^\circ 59' 20''\text{N}$  and  $103^\circ 19' 44''\text{E}$ .

A detailed analysis of the modification of the spatial distribution of TEC anomalies of seismic nature during this earthquake was performed in [Ruzhin et al., 2014]. It was shown that the TEC anomaly spot in the southern hemisphere is not a projection of the main spot (near the earthquake epicenter) produced along the geomagnetic field lines. As follows from the basic physical assumptions, the additional electric field must be transferred to the magnetically conjugated hemisphere without distortion due to the high longitudinal conductivity of the ionosphere. The resulting drift should create a similar result in plasma redistribution both above the earthquake preparation zone and in the magnetically conjugated ionosphere. Nevertheless, it is shown in [Ruzhin et al., 2014] that, in addition to the absence of the expected symmetrical position of the TEC anomaly relative to the magnetic equator, the anomaly centers in different hemispheres are located on opposite sides of the magnetic meridian passing through the earthquake epicenter (in the north to the east of it, and in the south – to the west, Figure 1).

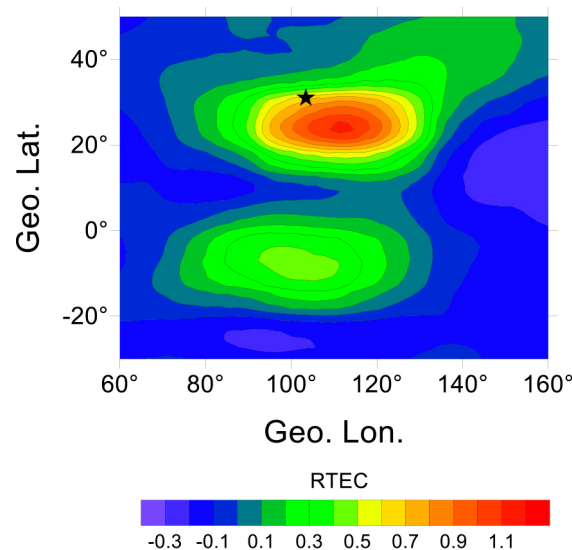


**Figure 1.** Relative total electric contents (RTEC) maps of the Chinese earthquake (May 12, 2008). RTEC anomaly is given in relative units. The epicenter location ( $31^\circ\text{N}$ ,  $103.4^\circ\text{E}$ ) is denoted by the asterisks [Ruzhin et al., 2014].

## A model of TEC perturbations possibly related to seismic activity

The main source of such anomalies in the ionosphere is considered to be an additional electric field that appears in the ionosphere above the preparation area of the impending earthquake. The plasma transfer in the direction of its drift caused by this additional field should create both areas of reduced and increased TEC disturbances. The developed model [Zolotov et al., 2008] does not explain the existence of an anomaly of the same sign and the observed asymmetry in the location of anomaly areas in magnetically conjugated regions relative to the geomagnetic meridian. Consequently, the above-mentioned mechanism of TEC disturbance formation as a result of plasma drift in an electric field cannot explain the results of the observation. It is obvious that it is necessary to take into account other processes in the ionosphere that accompany the appearance of an electric current and determine its source in the lithosphere.

At the same time, an injection of charged aerosols into the atmosphere in the epicentral region of an earthquake was detected, which results in occurrence of an electromotive force (EMF) in the surface layer of the atmosphere, which initiates a perturbation of the electric current in the global electric circuit and the appearance of an electric field in the ionosphere [Sorokin et al., 2007].

In this paper we present a physical model that describes the TEC disturbance as a result of heating the ionosphere by electric current and plasma drift in the electric field of this current. In this case, the spatial distribution of TEC arises as a result of the combined action of these two factors, and its nature will depend on the relationship between them. The developed model makes it possible to calculate the spatial distribution of TEC in the ionosphere for a given horizontal distribution of the concentration of charged aerosols in the atmosphere near the Earth's surface that may be used as a part of the complex method of the short-term prediction of earthquakes.

## 2. Analysis of results of observations of the electric field in the ionosphere

For the first time, quasi-static electric fields with an amplitude of about 10 mV/m, probably associated with the earthquake preparation, were discovered during the analysis of records of the vertical component of the electric field  $E_z$  obtained by the "Interkosmos-Bulgaria 1300" satellite (IKB-1300), whose trajectory altitude was 800 to 900 km [Chmyrev et al., 1989]. These electric fields were observed 15 minutes before the earthquake with magnitude  $M = 4.8$ , which occurred on January 12, 1982 at 17:50:26 UT in the Pacific Ocean with geographic coordinates 3.39°S, 177.43°E of the earthquake epicenter at a depth of 33 km. The perturbation of the quasi-static electric field with a value of 3 to 7 mV/m was observed in two areas at 17:38:00 UT above the earthquake epicenter and in the magnetically conjugated zone at 17:35:15 UT. Since the satellite moved from north to south, an increase in the electric field was noted first in the conjugate region, and then in the area above the earthquake epicenter. The horizontal size of the disturbed areas was approximately 1.5° in latitude. In the northern hemisphere, the electric field surge area is shifted to the south, and in the southern hemisphere – to the north relative to the areas of intersection of the disturbed magnetic tube with the lower ionosphere. In the southern hemisphere, this region coincides with the projection of the earthquake epicenter onto the lower ionosphere. The position of the disturbed electric field zones coincides with the areas where the satellite crosses the perturbed magnetic tube at the altitude of its trajectory. It was shown that the observed electric and magnetic fields are most likely related to the earthquake and are not the fields of ionospheric or magnetospheric origin. Further, detailed studies of quasi-static fields based on direct satellite measurements over seismically active regions of the globe were carried out in [Gousheva et al., 2006; Gousheva et al., 2008a; Gousheva et al., 2008b; Gousheva et al., 2009]. Hundreds of seismic events have been analyzed in order to isolate the associated anomalous enhancement of the electric field in the ionosphere. These studies consider seismic sources of different magnitudes in different tectonic settings at different latitudes. The orbits were selected with a distance of less than 25° to the earthquake epicenter, not crossing the terminator, as well as the time periods with a magnetic activity index  $K_p < 5$ . The paper [Gousheva et al., 2008b] presents the results of registration of electric fields on the IKB-1300 satellite in adjacent areas 11 to 13 hours before the earthquakes that occurred on August 25, 1981 ( $M = 5.2$  and  $M = 5.1$ , with the same hypocenter depth of 33 km) at 16:54:39 UT and 17:29:07 UT, respectively. At the same time, the geomagnetic activity index was  $K_p = 3$ , and the perturbations of the quasi-static electric field component  $E_z$  were 5 to 10 mV/m. The results of registration of the electric field on the IKB-1300 satellite 33 hours before the  $M = 5.0$  earthquake that occurred on August 23, 1981 at a depth of 10 km at 23:45:28 UT are given in [Gousheva et al., 2008b]. The index of geomagnetic activity was  $K_p = 3$ , and the perturbation of the  $E_z$  component of the quasi-static electric field above the trend was 26 mV/m. In this case, the area of disturbance was shifted to the north of the earthquake epicenter. The investigation of electric fields

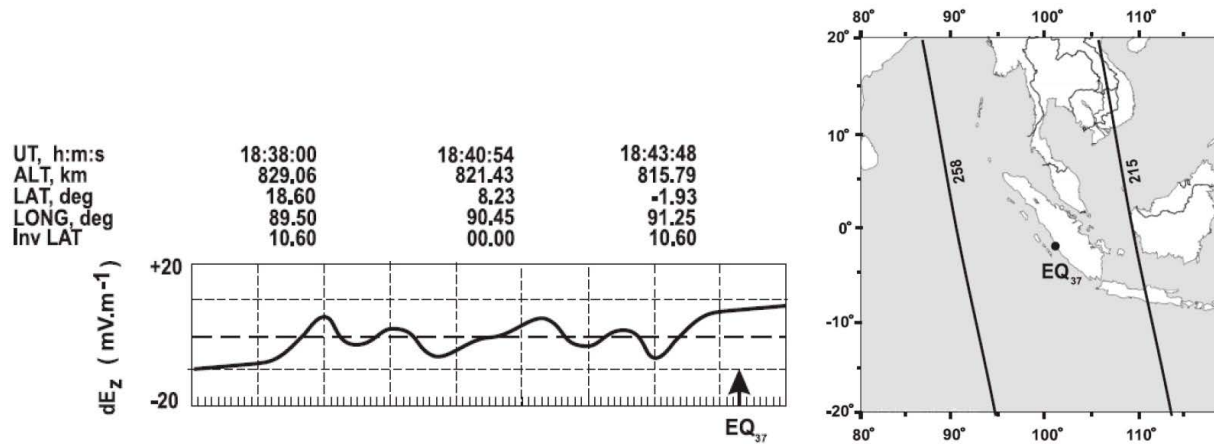


**Figure 2.** Disturbance of  $E_z$  component of the quasi-static electrical field for the orbit 258 [modified from Gousheva et al., 2009] (left panel). The arrow indicates the moment when the satellite flew at the closest distance from the earthquake epicenter.

on the IKB-1300 satellite in adjacent areas 85 hours before the earthquake ( $EQ_{37}$ ) with  $M = 4.9$  was performed in [Gousheva et al., 2009]. Earthquake was occurred on August 29, 1981 at 07:41:51 UT at a depth of 57 km. The results of registration are presented on Fig. 2. The index of geomagnetic activity was  $K_p = 3$ , and the perturbation of the  $E_z$  component of the quasi-static electric field above the trend was 6 mV/m.

Statistical analysis of the satellite data, carried out in the above-mentioned papers [Gousheva et al., 2008b; Gousheva et al., 2009], gave the authors reason to conclude that there is a source of a seismic nature for occurrence of the quasi-static electric field in the ionosphere. The duration of the electric field disturbance in the ionosphere with amplitude of about 10 mV/m can be up to 15 days. The amplitude of the electric field perturbation for the cases of observation at night and daytime in the ionosphere was of the same order.

Studies of the effect of seismic activity on electric field disturbances in the ionosphere were also carried out in [Zhang et al., 2012; Zhang et al., 2014]. The data of the DEMETER satellite obtained during the preparation of earthquakes with  $M = 7.1$  in the Yushu region of the Tibet Autonomous Region on April 13, 2010,  $M = 7.5$ , on the Nicobar Islands in the Indian region on July 12, 2010, and  $M = 7.2$  on Haiti on January 12, 2012 were analyzed. As an example, we present the data of registration of the electric field on the DEMETER satellite during the earthquake in Haiti, which occurred on January 12, 2012 at 16:53 LT. For analysis, the orbits were selected a week before this earthquake at a distance of 2000 km from its epicenter. It is shown that for orbit 29550-1 from 01/09/2012, 3 days before the earthquake in Haiti, a disturbance of the electric field components was observed to the north of the epicenter with an increase in its amplitude to 4 mV/m and 9 mV/m with a duration of about 40 s. In addition, a change in the signal shape was recorded on January 11, 2010 to the north of the earthquake epicenter along the orbit 29579-1. The disturbance amplitudes were 3.5 mV/m and 6 mV/m. Since the duration of the electric field disturbance was approximately 2 minutes, according to the satellite velocity of 8 km/s, the horizontal spatial scale was 900 km. Along with the satellite monitoring of the ionosphere over seismically active regions, the behavior of the electric field on the Earth's surface before earthquakes is analyzed [Vershinin et al., 1999; Hao et al., 1998; 2000; Rulenko, 2000; Smirnov, 2020]. It was shown that during the preparation of an earthquake, short local bursts of an electric field of large amplitude up to several kV/m with a duration of a few to tens of minutes occur. At the same time, there are no obvious perturbations of the electric field exceeding the background values, with duration of several hours and days, observed simultaneously at horizontal distances of tens and hundreds of kilometers in the seismic region.

Electric field disturbances similar to those observed over seismically hazardous regions were also detected by the “Kosmos-1809” satellite in the ionosphere above sea storms and typhoons [Isaev et al., 2002]. An increase in the electric field in the low-latitude ionosphere associated with the preparation and development of tropical storms and typhoons has been established. The electric field strength in this case reached  $\sim 20$  mV/m, which is anomalously high for the low-latitude ionosphere. Measurements of the electric field onboard the “Kosmos-1809” satellite during a strong tropical storm on January 17, 1989, were carried out at an altitude of  $\sim 950$  km. The maximum value of the electric field strength is 15-20 mV/m. In this case, the dimensions of the atmospheric disturbance should be 600-800 km, which corresponds to the ground-based observations. Simultaneous measurements of three

components of the quasi-static electric field, plasma density, and its fluctuations in the ionosphere were carried out on the “Kosmos-1809” satellite [Sorokin et al., 2005a]. The measurements were carried out over the area of typhoon HARRY, which was observed in the southwestern part of the Pacific Ocean from February 7 to February 13, 1989. Records of two components of the electric field in the horizontal plane were obtained, as well as the plasma density and its variations near the region of development of the typhoon on February 10, 1989. The maximum value of the electric field strength is 15-20 mV/m. Observations have shown that electric field disturbances are accompanied by an increase in the plasma density up to 20% relative to the background values and the appearance of small-scale plasma density fluctuations with a relative value of  $dN_e/N_e \sim 8\%$ .

### 3. Possible lithospheric sources of the electric field in the ionosphere

To find the physical connection between the TEC disturbance and the earthquake preparation processes, it is necessary to determine the possible source of the electric field that affects the ionosphere. The paper [Molchanov et al., 2004] presents the concept of the mechanisms of generation of phenomena in the atmosphere and ionosphere associated with the earthquake preparation. In the process of preparing the earthquake, fluid comes out to the earth's surface. Here, fluid is considered as a convective flow of water, gas, and heat in the lithosphere. The main ways of the fluid migration are tectonic faults. The authors believe that the migration of deep fluid bubbles can displace hot water and gas up to the ground surface and cause earthquakes in their preparation area. Disturbances in the temperature and density of the atmosphere increase as a result of the rise of hot water and gas before the earthquake. Soil gases carry charged soil aerosols into the atmosphere. Aerosol parameters can be obtained using satellite imagery or ground-based observations.

An increase in the density of charged aerosols by one or two orders of magnitude and an increase in the radioactivity of the atmosphere in seismically active regions were observed during the days and weeks before the earthquake due to the emission of radon and other radioactive substances [Alekseev and Alekseeva, 1992; Virk and Singh, 1994; Voitov and Dobrovolsky, 1994; Pulnits et al., 1997; Yasuoka et al., 2006; Omori et al., 2007; Biagi, 2009]. Data on the emission of soil gases, such as radon, helium, hydrogen, carbon dioxide in a seismically hazardous area ~500 km in diameter in the period from several hours to several weeks before the earthquake were presented in [King, 1986]. The paper [Boyarchuk, 1997] describes significant emissions of metal aerosols Cu, Fe, Ni, Zn, Pb, Co, Cr, and radon.

The concentration of aerosols in the surface layer is characterized by the Aerosol Optical Depth (AOD) parameter. This parameter is calculated from satellite data on the absorption of solar radiation with a wavelength of 550 nm of the visible spectrum reflected from the Earth's surface. The purpose of the research is to detect possible changes in the atmospheric AOD associated with earthquakes using the MODIS data obtained on the Terra and Aqua satellites [Akhoondzadeh et al., 2016]. The authors [Qin et al., 2014], using AOD data, demonstrated a significant change in aerosol concentration that appeared seven days before the Wenchuan earthquake (Wenchuan province, China, December 05, 2008). The AOD enhancement along the Longmenshan fault occurred 1 day and 4 days earlier than negative and positive ionospheric disturbances, respectively, and 1 day earlier than atmospheric anomalies, including air temperature, outgoing longwave radiation, and relative humidity. The authors [Okada et al., 2004] found significant changes in aerosol parameters before and after the catastrophic earthquake in the Gujarat province, India ( $M_w$  7.6, January 26, 2001). The correlation of aerosol injection into the atmosphere and other anomalies observed during the preparation of the earthquake in Chile ( $M_w$  8.8, February 27, 2010) was obtained in [Akhoondzadeh, 2015]. Aerosol parameters were analyzed on the basis of AOD satellite data, and the results of their analysis were compared with the data of registration of GPS-TEC anomalies, ion and electron densities, electron temperature, and ULF electric field. All these parameters and AOD data indicate their clear anomalous increase in the obtained time series for several days before the earthquake.

It was noted above that the release of soil gases in a seismic region increases during the earthquake preparation [King, 1986]. The intensification of these processes is observed on land near faults. Similar processes take place in the vicinity of underwater faults. Thus, direct observations revealed an intense rise of gas bubbles in the marine environment [McCartney and Bary, 1965; Lyon, 1972]. The presence of an electric charge of gas bubbles in the marine environment results in an appearance of a charged double layer near the surface of the bubble at the air-water interface. The shells of gas bubbles in water are negatively charged. The bubble charge is  $(10^{-14} - 10^{-15})$  Cl [Gak, 2013]. As a result of the bubble rising and bursting, the surface of its double charged layer sharply shrinks and two types of droplets are released into the atmosphere: small and larger. Small droplets are the remnants of

the surface film of the bubble that were in contact with the atmosphere. Larger droplets fly out from the bottom of the bubble. Large droplets with a larger mass soon fall back into the water, and the remaining, much smaller film droplets form aerosols in the atmosphere. It should be noted that when air bubbles burst, an electric charge is transferred to the atmosphere [Harper, 1957; Blanchard, 1963].

Thus, soil gas carries aerosols into the atmosphere, both over land and over the sea. Consequently, their impact on the atmosphere and possible connection with electrodynamic processes in the surrounding space is of a similar nature. This is confirmed by the fact that the disturbance of the electric field is observed on satellites for both continental and underwater earthquakes.

#### 4. A model for electric field formation in the ionosphere over seismic region

A detailed analysis of models for the occurrence of an electric field in the ionosphere is given in the review [Sorokin and Hayakawa, 2013]. The change in the quasi-static electric field in the ionosphere over the seismic region can be obtained in two ways. First, we can change the load resistance in the global electric circuit. About 80% of the resistance of this load is concentrated in the lower atmosphere, which is influenced by the processes of earthquake preparation. This resistance is changed as a result of the injection of radioactive, chemically active substances, aerosols into the atmosphere and variation in the atmosphere conditions. It has been shown that radon emissions into the atmosphere can change its conductivity by tens of percent [Omori et al., 2008; Harrison et al., 2010; Surkov, 2015], while they do not affect the electric field in the ionosphere. Calculations of the electric field penetration into the ionosphere, performed in [Kim and Hegai, 1999; Pulinets et al., 2000; Pulinets, 2009; Denisenko et al., 2008] showed that its value is orders of magnitude smaller than the background value in the ionosphere. Another possibility for the formation of an electric field in the ionosphere is the inclusion of an additional EMF in the global electric circuit. When an external EMF source is included in the global circuit, the vertical current in the atmosphere and the electric field in the ionosphere are changed. This model and the theory based on it for calculating the electric field are described in [Sorokin and Hayakawa, 2014; Sorokin et al., 2015; Sorokin et al., 2020] and references therein. In the electrodynamic model of lithosphere-atmosphere-ionosphere (LAI) coupling, the source of EMF is the injection of charged aerosols into the atmosphere. The EMF area is formed in the surface layers of atmosphere and includes the “lithosphere-atmosphere” interface. In this case, the observed electric field on the Earth’s surface is inside the EMF area. The external EMF current decreases with the altitude, while the conduction current increases. Here, the total current in the circuit does not change with the altitude. The conduction current at the Earth’s surface can be of the order of the fair-weather current, and the external current can exceed its value by four to five orders of magnitude. Since the current in the global circuit is continuous, the conduction current density in the ionosphere will be of the order of the external current density near the Earth’s surface. The horizontal component of the electric field  $E_1 \sim 10$  mV/m corresponds to the conduction current with a density  $j \sim \sigma_1 E_1 \sim 10^{-8}$  A/m<sup>2</sup>, where  $\sigma_1$  is the ionosphere conductivity. The conduction current near the Earth’s surface is  $10^{-12}$  A/m<sup>2</sup>, and the electric field  $E_1 \sim 100$  V/m. This fact may be illustrated by simple estimation. The continuity equation for the total current in the atmosphere has the form:

$$\nabla \times (\sigma \mathbf{E} + \mathbf{j}_{\text{ext}}) = 0, \quad (1)$$

where  $\mathbf{j}_{\text{ext}}$  is the external EMF current. An estimate of the electric field  $E_1$  in the ionosphere for the 1-D case gives  $\sigma_0 E_0 + j_{\text{ext}0} = \sigma_1 E_1$ . From this equality we derive  $E_1 = E_0(\sigma_0/\sigma_1)(1 + j_{\text{ext}0}/\sigma_0 E_0)$ , where  $j_{\text{ext}0}$ ,  $E_0$  – external EMF current density and electric field strength near the Earth’s surface, correspondingly;  $\sigma_0$  – conductivity of the lower atmosphere. If, for example, we assume that the external current is due to the movement of aerosols with a concentration  $N$ , charged by a charge  $Z_e$  under an action of vertical convection of the atmosphere at a speed  $v$ , then its value can be estimated by the formula  $j_{\text{ext}0} \approx Z_e N v$ . The charge of aerosols in atmosphere is in the range of  $100e$  to  $1000e$ . If we assume that  $Z = 3 \times 10^2$ ;  $N = 8 \times 10^9$  m<sup>-3</sup>;  $v = 0.3$  m/s, then we obtain an estimate of the electric field in ionosphere  $E_1 \approx 10^{-6}(1 + 10^4)$ V/m  $\approx 10$  mV/m. Even such a rough estimate shows that the model of electric field penetration into ionosphere should be based on the inclusion of EMF in the global electrical circuit. The EMF occurrence is possible in the process of intensification of the release of charged soil aerosols from the lithosphere into the atmosphere or changes in meteorological conditions with their stable altitude distribution.

### A model of TEC perturbations possibly related to seismic activity

The quasi-static altitude distribution of aerosols can be formed as a result of their turbulent upward transport and gravitational settling. Turbulent transfer is carried out due to the vertical gradient of the horizontal wind when the kinetic energy of the wind is converted into the energy of turbulent pulsations, as well as the thermal instability of the atmosphere in the case when the negative temperature gradient exceeds its adiabatic gradient. Turbulent vortices carry aerosols from the region of altitudes where their concentration is high to altitudes with their low concentration. Equilibrium is reached when the vertical flow of aerosols is balanced by their gravitational settling. For the first time, this model made it possible to explain the results of observing the disturbance of a quasi-static electric field in the ionosphere with a value of up to 10 mV/m and, at the same time, the absence of its noticeable disturbance on the Earth's surface in the seismic region.

Let us find the horizontal distribution of conductivity current in the ionosphere generated by external electric current located in the near ground atmosphere. We will use the Cartesian co-ordinates  $(x, y, z)$  with  $z$ -axis directed vertically upward and  $x$ -axis lying in magnetic meridian plane,  $a$  is the magnetic field inclination. At altitude  $z = z_1$  there is a thin conducting layer of the lower ionosphere. The plane  $z = 0$  coincides with the Earth's surface. The model used for calculations of current and electric field in the atmosphere-ionosphere electric circuit is presented in Figure 3.

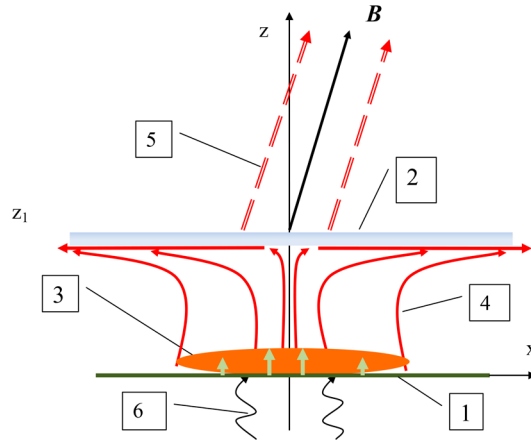


**Figure 3.** The model used for calculations of current and electric field in the atmosphere-ionosphere electric circuit above seismically active faults: 1. Earth surface. 2. Conductive layer of the ionosphere. 3. External electric current in the lower atmosphere above seismically active faults. 4. Conductivity electric current in the atmosphere-ionosphere circuit. 5. Electric field-aligned electric current. 6. Charged aerosols injected into the atmosphere by soil gases.

Distribution of vertical component of external current in horizontal plane  $(x, y)$  is determined by the function  $j_{ext0}(x, y) = j_{ext}(x, y, z = 0)$ , the electric field is given by  $\mathbf{E} = -\nabla\varphi$  and  $\sigma(z)$  denotes the atmosphere conductivity in the layer  $0 < z < z_1$ . We assume that the electric field potential  $\varphi$  is zero on the Earth surface. Its distribution in the atmosphere is derived from the current continuity equation and the Ohm's law and satisfies the following equation:

$$\frac{d}{dz} \left[ \sigma(z) \frac{d\varphi}{dz} - j_{est}(x, y, z) \right] = 0. \quad (2)$$

This equation is true in the case when the horizontal scale of external current exceeds the characteristic vertical scale of atmospheric conductivity variations. Plane  $z = z_1$  coincides with thin conductive ionosphere characterized by integral conductivity tensor  $\hat{\Sigma}$ . In quasi-static approximation the magnetic field lines in the magnetosphere are equipotential. Consequently, the distributions of electric field potential in the ionosphere and the field-aligned current on its upper boundary are transferred into the magnetically conjugate region without changes. The field-aligned current flowing in the magnetosphere is closed by the conductivity current in the conjugate ionosphere and atmosphere. The boundary condition at  $z = z_1$  can be found by integration of the current continuity equation

over the conjugate regions of the ionosphere [Sorokin et al., 2005b]. Solution of satisfying the boundary condition at  $z = z_1$  and condition on the Earth surface  $\varphi|_{z=0} = 0$  has a form:

$$\begin{aligned} \varphi(x, y, z) &= \int_0^z \frac{j_{est}(x, y, z')}{\sigma(z')} dz' - j_1(x, y) \int_0^z \frac{dz'}{\sigma(z')}; \quad j_1(x, y) = \frac{1}{\rho} [\varepsilon(x, y) - \varphi_1(x, y)] \\ \varepsilon(x, y) &= \int_0^{z_1} \frac{j_{est}(x, y, z)}{\sigma(z)} dz; \quad \rho \int_0^{z_1} \frac{dz}{\sigma(z)} \end{aligned} \quad (3)$$

where:  $\varphi_1(x, y)$  is the electric field potential distribution in the ionosphere,  $j_1(x, y)$  is the conductivity electric current on the lower edge of the ionosphere inflowing from the atmosphere. This distribution is connected with horizontal component of the electric field and the conductivity current flowing in the ionosphere. In this equation  $\varepsilon$  and  $\rho$  mean the electromotive force of external current and the electrical resistance of unitary area column between the ground and the ionosphere. Using the solution (3) and the boundary condition at  $z = z_1$  yields approximate equation for electric potential distribution  $\varphi_1(x, y)$  in the ionosphere:

$$\left( \frac{1}{\sin^2 \alpha} \frac{\partial^2}{\partial x^2} + \frac{\partial^2}{\partial y^2} \right) \varphi_1(x, y) = -\frac{j_1(x, y)}{2\Sigma_p}, \quad (4)$$

where  $\alpha$  is the magnetic field inclination,  $\Sigma_p$  is the Pedersen's integral conductivity of the ionosphere. Spatial scale of the ionosphere potential distribution depends on the slope of geomagnetic field. Equations (3) and (4) are applicable for calculation of the electric fields induced by external current over seismically active faults with arbitrary distribution in horizontal plane and for any altitude dependence of the atmosphere electric conductivity in oblique magnetic field.

Horizontal distribution of the electric field potential in the ionosphere is derived from Eq. (4). Transferring of the independent variables from  $(x, y)$  to  $\xi = x \sin \alpha, y$  in this equation leads to 2D Poisson equation, which is solved by Green function method. This solution in variables  $(x, y)$  has a form:

$$\begin{aligned} \varphi_1(x, y) &= -\frac{1}{4\pi\Sigma_p} \int_{-\infty}^{\infty} \int_{-\infty}^{\infty} G(x - x', y - y') j_1(x', y') dx' dy' \\ G(x, y) &= \sin \alpha \ln \sqrt{x^2 \sin^2 \alpha + y^2} \end{aligned} \quad (5)$$

The components of electric field in the ionosphere are determined by formulas:

$$E_x(x, y) = -\partial \varphi_1(x, y) / \partial x; \quad E_y(x, y) = -\partial \varphi_1(x, y) / \partial y. \quad (6)$$

Substituting expression (5) to (6) we obtain horizontal components of DC electric field in the ionosphere:

$$\begin{aligned} E_x(x, y) &= \frac{1}{4\pi\Sigma_p} \int_{-\infty}^{\infty} \int_{-\infty}^{\infty} K_x(x - x', y - y') j_1(x', y') dx' dy'; \\ E_y(x, y) &= \frac{1}{4\pi\Sigma_p} \int_{-\infty}^{\infty} \int_{-\infty}^{\infty} K_y(x - x', y - y') j_1(x', y') dx' dy'; \\ K_x(x, y) &= \frac{x \sin^3 \alpha}{x^2 \sin^2 \alpha + y^2}; \quad K_y(x, y) = \frac{y \sin \alpha}{x^2 \sin^2 \alpha + y^2}. \end{aligned} \quad (7)$$

## A model of TEC perturbations possibly related to seismic activity

Let us assume that the external electric current over fault is formed by superposition of currents arising from the injection of positive and negative charged aerosols into the atmosphere:

$$j_{ext}(x, y, z) = j_p(x, y)s_p(z) - j_n(x, y)s_n(z); \quad s_p(z=0) = s_n(z=0) = 1. \quad (8)$$

Functions  $s_p(z), s_n(z)$  denote the altitude distributions of external currents. Substitution of (8) in (3) yields:

$$j_1(x, y) = \frac{1}{\rho} [j_p(x, y)k_p - j_n(x, y)k_n]; \quad E_{z0}(x, y) = \frac{1}{\sigma_0} [j_1(x, y) - j_p(x, y) + j_n(x, y)];$$

$$k_{p,n} = \int_0^{z_1} dz \frac{s_{p,n}(z)}{\sigma(z)}; \quad E_{z0}(x, y) = E_z(x, y, z=0); \quad \sigma_0 = \sigma(z=0). \quad (9)$$

The atmospheric electric field variations at the distances within tens to hundreds km from earthquake center during seismically active period never exceed the background magnitudes  $\sim 10$ - $100$  V/m. The mechanism of feedback between disturbances of vertical electric field and the causal external currents near the Earth surface can explain such limitation [Sorokin et al., 2005a]. The feedback is caused by the formation of potential barrier on the ground-atmosphere boundary at the passage of upward moving charged aerosols through this boundary. Their upward transport is performed due to viscosity of soil gases flowing into the atmosphere. If, for example, positively charged particle goes from ground to the atmosphere, the Earth surface is charged negatively. The excited downward electric field prevents of particle penetration through the surface. At the same time this field stimulates the going out on the surface of the negatively charged particles. In a presence of such coupling the magnitudes of external currents on the Earth surface depend on vertical component of the electric field on the surface [Sorokin et al., 2005b]:

$$E_{z0}(x, y) = \frac{1}{\sigma_0} \left[ j_{p0}(x, y) \left( \frac{k_p}{\rho} - 1 \right) \sqrt{1 + \frac{E_{z0}(x, y)}{E_c}} - j_{n0}(x, y) \left( \frac{k_n}{\rho} - 1 \right) \sqrt{1 - \frac{E_{z0}(x, y)}{E_c}} \right]. \quad (10)$$

This equation allows calculating the vertical electric field component on the Earth surface at the given values of  $j_{p0}, j_{n0}$ . Critical field  $E_c$  may be estimated from the balance between viscosity, gravity and electrostatic forces. Equation (11) allows us to obtain the horizontal distribution of conductivity current on lower edge of the ionosphere inflowing from the atmosphere with accounting the feedback mechanism in following form:

$$j_1(x, y) = \frac{1}{\rho} \left[ j_{p0}(x, y) \sqrt{1 + \frac{E_{z0}(x, y)}{E_c}} k_p - j_{n0}(x, y) \sqrt{1 - \frac{E_{z0}(x, y)}{E_c}} k_n \right]. \quad (11)$$

Equations (7), (10) and (11) were used for computation of horizontal distribution of the electric field in the ionosphere and on the ground at different angles  $\alpha$  of inclination of the magnetic field and angles of orientation of the fault axis relatively to magnetic meridian plane. For the numerical calculations we assume that the model spatial distribution of external currents on the Earth's surface over fault is given by ellipse with the angle  $\beta$  of orientation of the fault axis relatively to magnetic meridian plane and the spatial scales of external current along  $a$  and across  $b$  the fault axis. We also assume  $s_{p,n} = \exp(-z/h_{p,n}); \sigma(z) = \sigma_0 \exp(z/h)$  and  $k_{p,n}/\rho = h_{p,n}/(h + h_{p,n})$ . Spatial distributions of DC electric field in the ionosphere and the vertical electric field on the Earth's surface for the same spatial structure of external current are presented in Fig. 4. The following parameters were used for numerical calculations:  $h_p = 20$  km;  $h_n = 15$  km;  $h = 5$  km;  $a = 500$  km;  $b = 100$  km;  $N_{p0} = 2 \times 10^{10} \text{ m}^{-3}$ ;  $\sigma_0 = 2 \times 10^{-14} \text{ S/m}$ ;  $\Sigma_p = 2 \text{ S}$ ;  $E_c = 450 \text{ V/m}$ .

These two figures show that at the selected parameters the horizontal electric field in the ionosphere reaches  $\sim 10$  mV/m, while the vertical electric field on the Earth's surface is limited by magnitude  $\sim 90$  V/m over active fault. Other important result is that DC electric field in the ionosphere has maximal magnitudes at the edges of area of external current. The horizontal scale of vertical electric field enhancement on the ground exceeds the characteristic horizontal scale of external current. Within this area the vertical field practically does not depend on distance.

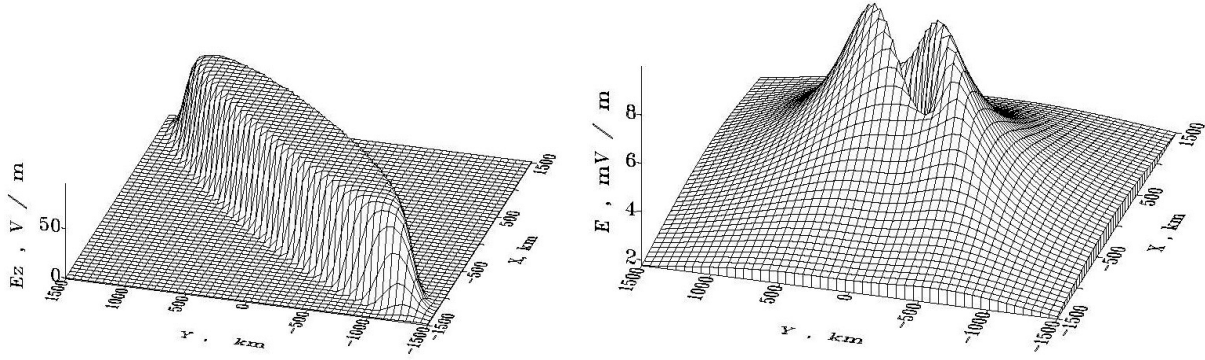


**Figure 4.** Spatial distribution of DC electric field calculated for the angle  $\beta = 45^\circ$  of orientation of the fault axis relatively to magnetic meridian plane [Sorokin et al., 2005b]. Left panel: Vertical component of DC electric field on the ground. Right panel: Horizontal component of DC electric field in the ionosphere. Angle of magnetic field inclination is  $20^\circ$ .

In the study [Ruzhin et al., 2014] the results of the above research were used to estimate the horizontal distribution of the electric field in the ionosphere. Since the longitudinal component of the ionosphere conductivity significantly exceeds its transverse components, the potential distribution in the horizontal plane  $\varphi_1(x, y)$  at the lower boundary of ionosphere  $z = z_1$  is transferred without change along the geomagnetic field lines to the upper ionosphere and at an arbitrary altitude  $z > z_1$  is determined by the expression:

$$\varphi(x, y, z) = \varphi_1\left(x - \frac{z - z_1}{\tan\alpha}, y\right).$$

The potential  $\varphi_1(x, y)$  is determined from equation (6). The external EMF current in the surface layer of the atmosphere  $j_{ext} = j_p - j_n$  is formed by currents of positively charged  $j_p$  and negatively charged  $j_n$  aerosols. Electric current  $j_1(x, y)$  is connected with these currents by equation (11). In the study [Ruzhin et al., 2014] the following estimate of the current of positively and negatively charged aerosols near the Earth surface was used:

$$j_{p0}(x, y) = (Ze\sigma_0/\varepsilon_0)h_p N_{p0}(x, y); \quad j_{n0}(x, y) = (Ze\sigma_0/\varepsilon_0)h_n N_{n0}(x, y), \quad (12)$$

where:  $e$  - elementary charge,  $\varepsilon_0$  - electrical constant,  $Z$  - a number of elementary charges on aerosols,  $N_{p0, n0}$  - concentration of positively and negatively charged aerosols on the Earth's surface. The results of observations confirm an absence of noticeable variations of quasi-static electric field in the seismically active region. Therefore, for a simple assessment of the electric field in the ionosphere, we may assign  $E_{z0} = 0$ . This approximation was used in [Ruzhin et al., 2014]. In this case, using equations (12), (13), and (14), we obtain a relationship between the density of the atmospheric electric current at the lower boundary of the ionosphere and the concentration of positively charged aerosols on the Earth's surface:

$$j_1(x, y) = \frac{Ze\sigma_0 h_p (h_p - h_n)}{\varepsilon_0 (h + h_p)} N_{p0}(x, y). \quad (13)$$

The following spatial distribution of aerosol concentration on the Earth's surface was chosen for calculations:

$$N_{p0}(x, y) = N_0 \exp\left(-\frac{x^2}{l_x^2} - \frac{y^2}{l_y^2}\right).$$

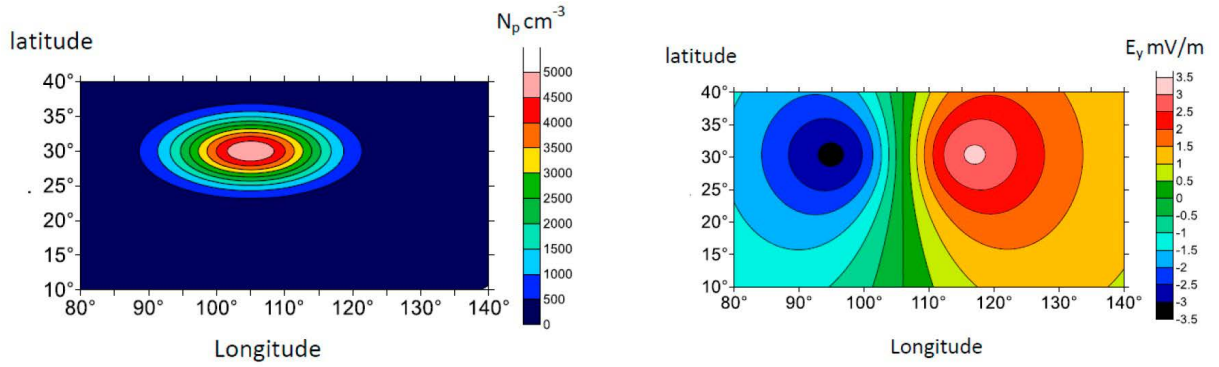


**Figure 5.** Left panel: Spatial distribution of the concentration of positively charged aerosol particles on the Earth’s surface. Right panel: Horizontal distribution of the zonal component of the electric field in the ionosphere.

The left panel of Fig. 5 shows the spatial distribution of aerosols obtained by the formula above for  $N_0 = 5 \times 10^9 \text{ m}^{-3}$ ,  $l_x = 500 \text{ km}$ ,  $l_y = 1200 \text{ km}$ . The spatial distribution of aerosols shown in Figure 5 (left panel) was used for calculations of spatial distribution of the zonal component of the electric field disturbance in the ionosphere by formulas (9) and (15). An epicenter of the aerosol release (point  $x = y = 0$ ) was chosen at the point with coordinates (30°N; 105°E). In this case, the center of TEC disturbance is located at the point with coordinates (25°N; 115°E). Results of calculations are shown in Fig. 5 (right panel). The following parameters were used:  $\sigma_0 = 2 \times 10^{-14} \text{ S/m}$ ;  $\Sigma_p = 6 \text{ S}$ ;  $e = 1.6 \times 10^{-19} \text{ C}$ ;  $\epsilon_0 = 8.8 \times 10^{-12} \text{ F/m}$ ;  $Z = 100$ ;  $h_p = 5 \text{ km}$ ;  $h_n = 2 \text{ km}$ ;  $\alpha = 37^\circ$ .

For these parameters the maximal conduction current at the lower boundary of ionosphere is  $j_1 = 3.3 \times 10^{-7} \text{ A/m}^2$ . According to the plot (Fig. 5, right panel) the electric field disturbance obtains 3.5-4.0 mV/m. This value is consistent with the results of numerical simulations obtained in the studies listed above and observational data. Consequently, the considered model of lithosphere-ionosphere coupling may be applied to the study of the nature of TEC disturbances during periods of increased seismic activity.

## 5. Ionosphere heating by electric current

It should be noted that the appearance of an electric field in the ionosphere is resulted not only in the plasma drift in the F-layer. As shown in [Sorokin and Chmyrev, 1999], the electric field increase and associated rise of the heat released in the E-layer of the ionosphere as a result of the electric current in it leads to an increase in the temperature of the F-layer. This affects the processes forming the F-layer. The heat flux produced by electric current in the conducting layer of the ionosphere with integral conductivity  $\Sigma$  in a horizontal electric field of strength  $E$  is equal, in order of magnitude, to  $\lambda = \Sigma E^2$ . Assuming the values:  $\Sigma = 3\text{-}30 \text{ S}$ ,  $E = 6 \text{ mV/m}$ , we obtain  $\lambda = 10^{-4}\text{-}10^{-3} \text{ W/m}^3$ . One of the main sources of the ionosphere heating is the Sun’s short-wave radiation ( $<1026 \text{ \AA}$ ). The heat influx as a result of the absorption of this radiation at an altitude of over 100 km is approximately  $\lambda = 10^{-3} \text{ W/m}^3$  and, depending on the solar cycle, can change several times both up and down. From the above estimates it follows that the heat generated by the electric current in the ionosphere above the earthquake preparation zone constitutes a significant part of the total heat balance of the ionosphere. Consequently, this heat source has a decisive influence on its condition. The heating by ionospheric currents increases the scale of the altitude distribution of ionospheric components and, consequently, the scale of altitude profile of the F2-layer. At the altitudes above 200 km the ionosphere is isothermal (temperature of the ionosphere varies little with altitude). In the altitude range from 100 km to 200 km there is a positive gradient of temperature. Presence of this temperature gradient due to thermal conductivity results in the thermal flux directed downward. The source of Joule heating is located in the layer of 120 to 150 km of altitude. Therefore, a heating of the upper ionosphere layers can be realized only at a presence of gas movement in the vertical direction.

Following the study [Sorokin and Chmyrev, 1999], let’s determine the temperature of the upper ionosphere when an electric current flows in its conducting layer. We assume that the Joule heat of ionospheric currents is released in a thin conducting layer coincident with the  $(x,y)$ -plane at the altitude  $z = z_1$ . Magnetic field  $\mathbf{B}$  is directed along the  $z$ -axis. Since the disturbance region is considerably extended in the horizontal direction, let us assume that

the main variations of the quantities occur along the  $z$ -axis. In this case the stationary motion of gas arising due to action of the heat source in the planar-irregular layered ionosphere will be described by the system of hydrodynamic equations including the motion, continuity, the heat transfer equations, and the equation of state:

$$\begin{aligned} \rho v \frac{dv}{dz} &= -\frac{dP}{dz} \rho g, \quad \frac{d(\rho v)}{dz} = 0, \quad P = \left(\frac{k}{M}\right) \rho T, \\ c_p \rho v \frac{dT}{dz} &= \frac{d}{dz} \left[ k(T) \frac{dT}{dz} \right] + \lambda \delta(z - z_1) \end{aligned} \quad (14)$$

where  $\rho, P, T$  are the density, pressure and temperature of the atmosphere,  $v$  is the atmosphere velocity,  $M$  is the mass of molecule,  $\delta \times (z - z_1)$  is the Dirac delta function,  $g$  is the acceleration of gravity,  $c_p$  is the heat capacity at constant pressure,  $k$  is the Boltzmann constant, and  $\kappa(T) = \kappa_0 \sqrt{T/T_0}$  is the coefficient of thermal conductivity that depends on the temperature, where  $T_0$  is the atmosphere temperature near the ground. From continuity equation (14) we derive  $\rho v = I_0 = \text{const}$ . Using this equality and the equation system (14), we obtain:

$$\frac{d}{dz} \left[ c_p I_0 T - \kappa_0 \sqrt{\frac{T}{T_0}} \frac{dT}{dz} \right] = \lambda \delta(z - z_1). \quad (15)$$

Integrating (15) on  $z$  in the vicinity of  $z_1$  and assuming continuity of  $T(z)$ , we obtain the condition for a jump of the temperature gradient when crossing the  $z = z_1$  plane:

$$\left. \frac{dT}{dz} \right|_{z_1} - \left. \frac{dT}{dz} \right|_{z_1-0} = -\frac{\lambda}{\kappa_0} \sqrt{\frac{T_0}{T_1}},$$

where  $T_1$  is the ionosphere temperature at the altitudes  $z \geq z_1$ . The limited solution of equation (15) at  $T(z=0) = T_0$  has the form:

$$T(z) = T_0 \left( 1 + \frac{c_p I_0}{2\kappa_0} z \right)^2. \quad (16)$$

Substituting (16) in the boundary condition, we obtain:

$$\left( 1 + \frac{c_p I_0}{2\kappa_0} z_1 \right) \sqrt{\frac{T_1}{T_0}} = \frac{\lambda}{c_p I_0 T_0}. \quad (17)$$

Integration of equation (15) on  $z$  from 0 to  $z_1 + 0$  and using the formula (16) enables us to determine the relation between the mass and heat fluxes:

$$c_p I_0 T_1 = \lambda. \quad (18)$$

From equations (17) and (18) we derive the dependence of ionosphere temperature  $T_1$  on the thermal flux  $\lambda$ :

$$\frac{T_1}{T_0} \left( \sqrt{\frac{T_1}{T_0}} - 1 \right) = \frac{\lambda}{\lambda^*}; \quad \lambda^* = \frac{2\kappa_0 T_0}{z_1}. \quad (19)$$

Thus, the thermal energy injected in the  $z = z_1$  plane is transferred to the top region due to gas travel. In this process gas is gradually heated during its approach to the heat source. This process characterizes the thermal interchange

## A model of TEC perturbations possibly related to seismic activity

in the upper atmosphere and determines the temperature altitude distribution in this region. Approaching of  $\lambda$  to 0 corresponds to transition to the isothermal atmosphere  $T_1 \rightarrow T_0$  where the vertical mass transport is absent ( $I_0 = 0$ ).

The heat flow  $\lambda$  radiated by the surface electric current  $\hat{\Sigma}\mathbf{E}$ , flowing in the thin conductive layer of ionosphere in the inclined geomagnetic field is determined by formula:

$$\lambda = (\hat{\Sigma}\mathbf{E} \cdot \mathbf{E}) = \Sigma_p(E_x^2/\sin^2 \alpha + E_y^2),$$

where the tensor  $\hat{\Sigma}$  is (e.g., see [Sorokin et al., 2006]):

$$\hat{\Sigma} = \begin{pmatrix} \Sigma_p/\sin^2 \alpha & \Sigma_H/\sin \alpha \\ -\Sigma_H/\sin \alpha & \Sigma_p \end{pmatrix}$$

By substitution of equation (21) and (8) into (20) we obtain a dependence of the ionosphere temperature  $T_1$  on horizontal distribution of electric field potential  $\varphi_1$  in the conductive layer where the current flows:

$$\frac{T_1}{T_0} \left( \sqrt{\frac{T_1}{T_0}} - 1 \right) = \frac{\Sigma_p}{\lambda^*} \left[ \frac{1}{\sin^2 \alpha} \left( \frac{\partial \varphi_1}{\partial x} \right)^2 + \left( \frac{\partial \varphi_1}{\partial y} \right)^2 \right]. \quad (20)$$

The dependence of the ionosphere temperature  $T_1$  on the electric field in ionosphere is determined by equation (20). The ionosphere potential  $\varphi_1$  is calculated by formula (7) where the horizontal distribution of electric current  $j_1(x, y)$  is determined by equation (15). The corresponding horizontal distributions of aerosols on the Earth's surface and electric field in ionosphere are shown in Figure 5. Results of calculation of horizontal distribution of ionosphere temperature as a result of injection of aerosols into atmosphere are shown in Figure 6.

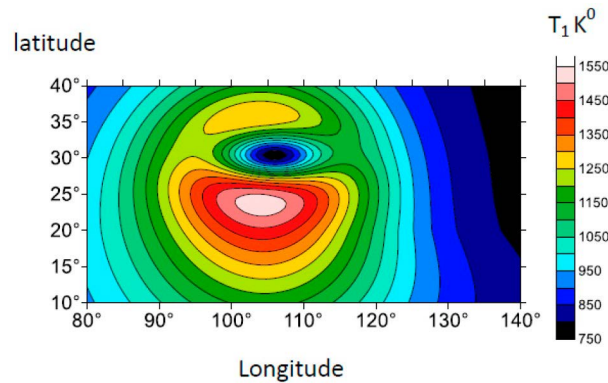


**Figure 6.** Horizontal temperature distribution of the ionosphere  $T_1$  (in Kelvin degrees) heated by electric current.

Assuming the air thermal conductivity with the normal conditions:  $\kappa_0 = 3 \times 10^{-2} \text{ W/m} \cdot \text{K}^0$ ,  $z_1 = 10^5 \text{ m}$ ,  $T_0 = 300\text{K}^0$ , we find  $\lambda^* = 2 \times 10^{-4}$ . For calculations the value  $\Sigma_p = 6 \text{ S}$  is selected. The heat release in E-layer results in the heating of F-layer of ionosphere and increase of its temperature. The ionosphere temperature increases over the area of heat release resulted in increase of a scale of vertical distribution of components of ionosphere. This modification of the ionospheric altitude profile leads to an increase in TEC in the entire disturbed region. Hence, the model of the ionosphere thermal balance based on the ionosphere heating by the vertical mass transfer due to the heat injection in its bottom layers enables to determine the temperature depending on the heat flux. This flux consists of the Joule heat of ionospheric currents flowing in the conducting layer.

## 6. A model for TEC disturbance as a result of injection of charged aerosols into the atmosphere

The modification of the TEC spatial distribution caused by the disturbance of the electric current in the global circuit as a result of the injection of charged aerosols into the atmosphere is considered in [Ruzhin et al., 2014]. The analysis was carried out for the case of the  $M_w$  7.9 earthquake that occurred on May 12, 2008 at 06:28 UT in Sichuan Province, China, and for which there is a detailed anomaly registration database. In addition, during the preparation of this earthquake, the release of aerosols into the atmosphere in the area of its epicenter was detected [Qin et al., 2014].

Let us consider a modification of the spatial distribution of electron concentration  $N$  in the ionosphere caused by a disturbance of the global electric current circuit in a seismic region. The TEC disturbance is determined by the plasma concentration of the F2-layer of the ionosphere in the altitude range of 200-1000 km. In the mid-latitude ionosphere, for TEC calculations it is sufficient to take into account only the vertical transport of charged particles due to the smallness of the horizontal derivatives of macroscopic parameters. As follows from the observation results, the horizontal scale of the ionosphere disturbance is about 1000 km, which significantly exceeds the vertical scale of the change in electron concentration.

An estimate was obtained for the TEC disturbance in an isothermal atmosphere that occurs under an influence of the vertical drift of F2-region plasma in the electric field and heating of the ionosphere by the same field [Ruzhin et al., 2014]. The electron concentration  $N(z)$  is determined from the stationary transport equation:

$$\frac{dJ(z)}{dz} = q(z) - \beta(z)N(z); \quad J(z) = -D(z) \left( \frac{dN}{dz} + \frac{N}{2H} \right) + wN, \quad (21)$$

where  $q(z)$  - ionization rate,  $\beta(z)$  - effective recombination factor,  $D(z) = k_B T / M v_{in}$  - ambipolar diffusion factor,  $H = k_B T / Mg$  - altitude of uniform atmosphere,  $k_B$  - Boltzmann constant,  $T$  - temperature of atmosphere,  $M$  - mass of ion and molecule,  $v_{in}$  - rate of collision of ions with molecules,  $g$  - gravitational acceleration. Vertical drift rate  $w$  of plasma under action of electrical field  $\mathbf{E}_0 + \mathbf{E}$  and neutral wind with velocity  $\mathbf{V}$  is determined by formula:

$$w = \left( \frac{E_{y0} + E_y}{B} \right) \cos \alpha + V_x \cos \alpha \sin \alpha,$$

where  $E_{y0}$ ,  $V_x$  - components of undisturbed electric field and horizontal wind,  $B$  - geomagnetic induction,  $E_1$  - electric field occurred in ionosphere as a result of EMF inclusion into the global electric circuit. The plasma drift rate may be represented in the following form:

$$w = w_0 + \frac{E_y}{B} \cos \alpha; \quad w_0 = \frac{E_{y0}}{B} \cos \alpha + V_x \cos \alpha \sin \alpha, \quad (22)$$

where  $w_0$  - undisturbed value of the drift rate under action of electric field and the wind of non-seismic nature.

The altitude dependence of ionization rate  $q(z)$  we represent in the form of Chapman's function. Over its maximum  $z \approx z_0$  this function is approximately proportional to density of neutral gas, which is atomic oxygen:

$$q(z) = q_0 \exp \left( -\frac{z - z_0}{H} \right).$$

Let us designate:  $T_0$  - temperature of ionosphere at an absence of its heating by electric current of seismic origin,  $H_0 = kT_0 / Mg$  - the altitude of uniform atmosphere that corresponds to temperature  $T_0$ . Designating the

## A model of TEC perturbations possibly related to seismic activity

relative change of temperature as  $t = T_1/T_0$ , we represent the dependence of ionization rate on the temperature in the following form:

$$q(z) = q_0 \exp\left(-\frac{z - z_0}{H_0 \tau}\right). \quad (23)$$

The ionization rate in the maximum  $q_0$  is varied within a range of  $10^8$ - $10^9 \text{ m}^{-3}\text{s}^{-1}$  depending on depending on the time of day and solar activity.

Let us integrate the equation (23) on  $z$  within a range from  $z_0$  to  $\infty$ , where  $z_0 \approx 200 \text{ km}$  – lower boundary of F2-layer. We obtain:

$$J_\infty - J(z_0) = Q - \bar{\beta}U; \quad Q = \int_{z_0}^{\infty} q(z)dz = q_0 H_0 \tau, \quad (24)$$

where  $J(z_0)$  – ion flow at the lower boundary of the F2-layer of the ionosphere,  $J_\infty$  – ion flow at its upper boundary,  $\bar{\beta} = \int_{z_0}^{\infty} \beta(z)N(z)dz / U$  – averaged recombination coefficient. In the equation (26)  $U$  denotes TEC, which is determined by formula:

$$U = \int_{z_0}^{\infty} N(z)dz. \quad (25)$$

When estimating the ion flux  $J(z_0)$  at the bottom boundary of the F2-layer the effect of ion diffusion is neglected and only considered the ion drift:

$$J(z_0) \approx wN(z_0) = w N_0.$$

From (26) we obtain the required TEC value:

$$U = \frac{q_0 H_0 \tau + w N_0 - J_\infty}{\bar{\beta}} \quad (26)$$

The value of the weighted average value of the recombination coefficient  $\bar{\beta}$  is determined from condition of coincidence of TEC calculated by formula (28) at an absence of disturbance of electric field by seismic source and its value  $U_0$  obtained by formula (27) with application of ionosphere model IRI-2007:

$$U_0 = \frac{q_0 H_0 + w_0 N_0 - J_\infty}{\bar{\beta}}. \quad (27)$$

We will look for a disturbance in the TEC associated with the appearance of an additional electric field  $E_y$  in ionosphere  $\Delta U = U - U_0$  relative to its unperturbed value  $U_0$ . Using the formula (24) for perturbation of the drift rate by additional electric field we obtain:

$$RTEC = \frac{\Delta U}{U_0} = \frac{q_0 H_0 (T_1/T_0 - 1) + (E_y/B) N_0 \cos \alpha}{q_0 H_0 + w_0 N_0 - \infty}. \quad (28)$$

The spatial distribution of TEC arises as a result of the combined action of these two factors and its nature depends on the relationship between them. The spatial distribution of the TEC disturbance resulting from the combined

effect of the vertical drift of the F-region plasma in the electric field and heating of the ionosphere by the same field is calculated by formula (28). The horizontal distribution of ionosphere temperature  $T_1$  occurring as a result of its heating by electric current is determined by formula (22). The results of its calculation are shown in Fig. 6. The horizontal distribution of the component  $E_y$  of electric field is calculated by formula (9). The results of its calculation are shown in Fig. 5 (right panel). Figure 7 shows the results of calculating the relative TEC (RTEC) disturbance. The graph in Fig. 7 was plotted for the ionization rate at the lower boundary of the F2-layer  $q_0 = 5 \times 10^8 \text{ m}^{-3}\text{s}^{-1}$ . The following values were taken for the calculation:  $N_0 = 3 \times 10^{11} \text{ m}^{-3}$ ,  $E_{0y} = 1.5 \text{ mV/m}$ ,  $B = 5 \times 10^{-5} \text{ T}$ ,  $H_0 = 10 \text{ km}$ .

At the upper boundary of the daytime ionosphere, the ion flux is directed upward and is approximately equal in magnitude  $J_\infty \sim 10^{12} \text{ m}^{-2}\text{s}^{-1}$  [Evans, 1975].

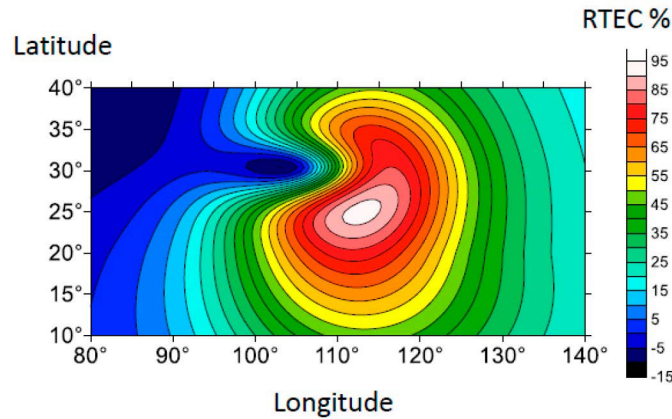


Figure 7. Spatial distribution of RTEC disturbance.

The calculations performed show that a change in the concentration of aerosols injected into the atmosphere results in the TEC perturbation of the ionosphere by tens of percent. This value corresponds to observed TEC variations of 40 to 100% before earthquakes [e.g., Namgaladze et al., 2009]. A diagram of TEC disturbance formation is shown in Fig. 8. The left panel of Fig. 8 (left) shows the direction of plasma drift ( $E \times B$ ) in an electric field. As follows from the figure, where the field is directed to the east, the plasma drift is directed upward. In the region where the field is directed to the west, the plasma drift is directed downward. The calculation results presented above showed that the field strength exceeds its background value in the ionosphere by several times. Consequently, the plasma drift in such field results in a significant TEC change.

The right panel of Fig. 8 shows a diagram of the TEC disturbance formation as a result of heating the ionosphere by the current flowing in its conducting layer. The temperature of the ionosphere increases above the region of heat

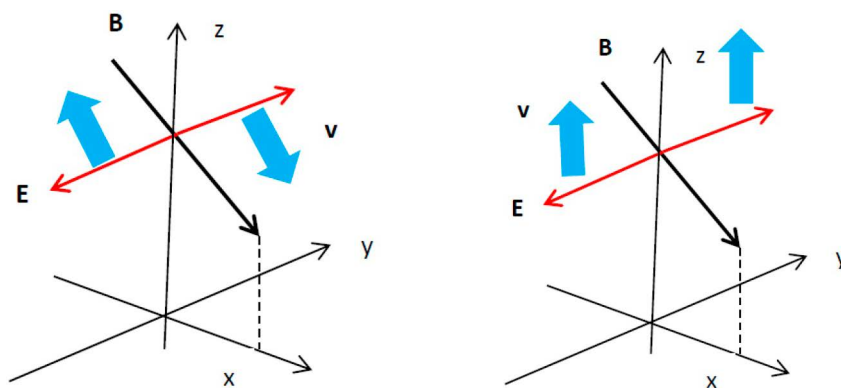


Figure 8. Scheme of TEC disturbance formation under the influence of plasma drift in an electric field (left) and its heating by current in the ionosphere (right) as a result of injection of charged aerosols into the atmosphere.

release, which leads to an increase in the scale of the vertical distribution of the ionospheric components. Since the heat flux is proportional to the square of the field, an anomaly of the same sign occurs. Such a modification of the altitude profile of the ionosphere leads to an increase in the TEC in the entire disturbed region. The spatial distribution of TEC arises as a result of the combined action of these two factors, and its nature depends on the relationship between them.

## 7. Conclusion

Observations demonstrate that TEC anomalies may be formed in the seismic region before an earthquake. There is a problem of establishing a connection between such anomalies and the processes of earthquake preparation. An analysis of numerous satellite data has shown that an increase in seismic activity results in an increase in the electric field in the ionosphere above the earthquake epicenter several days before the main shock. At the same time, there are no noticeable changes in the vertical component of the electric field on the Earth's surface in the seismic region. In addition, an increase in the concentration of aerosols in the epicentral region was detected using the analysis of Aerosol Optical Depth (AOD) satellite observation data. Numerical modeling showed that the observed changes in TEC are possible if the electric field in the ionosphere reaches a value of the order of 1 to 10 mV/m. The appearance of such fields in the ionosphere is explained by the electrodynamic model of lithospheric-ionospheric relations, which showed that an increase in the electric field in the "atmosphere-ionosphere" system is possible as a result of perturbation of the electric current in the global electric circuit during the injection of charged aerosols into the atmosphere by soil gases. As a result of their turbulent and convective transfer and gravitational settling in the surface atmosphere, an EMF is formed, the introduction of which in the global electric circuit results in a perturbation of the conduction current in it. The presence of a potential barrier during the injection of charged aerosols into the atmosphere limits the growth of the electric field on the earth's surface. The EMF occurrence triggers the mechanism of transmission of seismic activity to the ionosphere. The electric field is localized in the magnetic tube and causes the plasma to drift in a transverse plane with respect to the magnetic field. The plasma drift forms an anomaly in which regions of TEC increase and decrease are observed. The calculations performed using the electrodynamic model of lithospheric-ionospheric relations showed that an increase in the concentration of aerosols near the Earth's surface by several times results in the relative TEC change by tens of percent. The appearance of an electric current in the ionosphere is reduced not only to the plasma drift in the F-region. Its strengthening results in an increase in the amount of heat released in the conducting layer of the E-region of the ionosphere. The heat flow heats the F-region. As a result of an increase in the temperature of the ionosphere, the scales of the altitude distribution of ionospheric components and, consequently, the altitude profile of the F2-layer increase. This results in a spatial distribution of the TEC disturbance of the same sign. The heating of the ionosphere when an electric field  $E \sim 6$  mV/m appears in it results in a relative TEC change by the same value as the plasma drift in this field. The total spatial distribution of TEC arises as a result of the action of these two factors, and its nature depends on the relationship between them. Their combination can explain various forms of anomalies observed before earthquakes.

**Acknowledgement.** The study was supported by the Ministry of Science and Higher Education of the Russian Federation (State Assignments of IZMIRAN No. 01201356396, JIHT RAS No. 075-00270-24-00, and IDG RAS No. 122032900167-1).

## References

- Afraimovich, E.L., E.I. Astafieva, M.B. Gokhberg, V.M. Lapshin, V.E. Permyakova, G.M. Steblov and S.L. Shalimov (2004). Variations of the total electron content in the ionosphere from GPS data recorded during the Hector Mine earthquake of October 16, 1999, California, Rus. J. Earth Sci., 6, 339-354.
- Akhoondzadeh, M. (2015). Ant Colony Optimization detects anomalous aerosol variations associated with the Chile earthquake of 27 February 2010, Adv. Space Res., 55, 1754-1763.
- Akhoondzadeh, M. and F.J. Chehrebargh (2016). Feasibility of anomaly occurrence in aerosols time series obtained from MODIS satellite images during hazardous earthquakes, Adv. Space Res, 58, 890-896.

- Alekseev, V.A. and N.G. Alekseeva (1992). Investigation of metal transfer in the biosphere during gaseous emission in zones of tectonic activity using methods of nuclear physics, *Nucl. Geophys.*, 6, 99-105.
- Astafieva E. (2019). Ionospheric detection of natural hazards, *Rev. Geophys.*, 57, 1265-1288.
- Biagi, P.F. (2009). Pre and post seismic disturbances revealed on the geochemical data collected at Kamchatka (Russia) during the last 30 years, in *Electromagnetic Phenomena Associated with Earthquakes* M. Hayakawa (Editor), Transworld Research Network, Trivandrum, India, 97-117.
- Boyarchuk, K.A. (1997). Kinetics of elementary ions in the lower atmosphere acted upon by ionizing radiation, *Proc. Russian Acad. Sci., Atmos. Ocean. Phys.*, 33, 236-240.
- Blanchard, D.C. (1963). The electrification of the atmosphere by particles from bubbles in the sea, *Progress in oceanography*. McMillan Co., N.Y., 1, 73-197.
- Chmyrev, V.M., N.V. Isaev, S.V. Bilichenko and G.A. Stanev (1989). Observation by space-borne detectors of electric fields and hydromagnetic waves in the ionosphere over an earthquake center, *Phys. Earth Planet. Inter.*, 57, 110-114.
- Denisenko, V.V., M.Y. Boudjada, M. Horn, E.V. Pomozov, H.K. Biernat, K. Schwingenschuh, H. Lammer, G. Prattes and E. Cristea (2008). Ionospheric conductivity effects on electrostatic field penetration into the ionosphere, *Nat. Hazard. Earth Sys.* 8, 1009-1017.
- Evans, J.A. (1975). A study of F2 region daytime vertical ionization fluxes at Millstone Hill during 1969, *Planet. Space Sci.*, 23, 1461-1482.
- Harrison, R.G., K.L. Aplin and M.J. Rycroft (2010). Atmospheric electricity coupling between earthquake regions and the ionosphere, *J. Atmos. Solar-Terr. Phys.*, 72, 376-381.
- Harper, W.R. (1957). The generation of static charge. *Philos. Mag. Suppl. Adv. Phys.*, 6, 365-417.
- Hao, J.G., T.M. Tang and D.R. Li (1998). A kind of information on short-term and imminent earthquake precursors – research on atmospheric electric field anomalies before earthquakes, *Acta Seismol. Sin.*, 11, 121-131.
- Hao, J., T. Tang and D. Li (2000). Progress in the research of atmospheric electric field anomaly as an index for short-impending prediction of earthquakes. *J. Earthquake Pred. Res.*, 8, 241-255.
- Gak, E.Z. (2013). Magnetic fields and aqueous electrolytes in nature, scientific research and technologies, Elmor, Saint-Petersburg, 343-364 (in Russian).
- Gousheva, M.N., R.P. Glavcheva, D.L. Danov, P. Angelov, P.L. Hristov, B.B. Kirov and K.Y. Georgieva (2006). Satellite monitoring of anomalous effects in the ionosphere probably related to strong earthquakes, *Adv. Space Res.*, 37, 660-665.
- Gousheva, M.N., R.P. Glavcheva, D.L. Danov, P.L. Hristov, B.B. Kirov and K.Y. Georgieva (2008a). Electric field and ion density anomalies in the mid latitude ionosphere: Possible connection with earthquakes? *Adv. Space Res.*, 42, 206-212.
- Gousheva, M.N., D.L. Danov, P. Hristov and M. Matova (2008b). Quasi-static electric fields phenomena in the ionosphere associated with pre- and post earthquake effects, *Nat. Hazard. Earth Sys.*, 8, 101-107.
- Gousheva, M.N., D.L. Danov, P. Hristov and M. Matova (2009). Ionospheric quasi-static electric field anomalies during seismic activity August-September 1981, *Nat. Hazard. Earth Sys.*, 9, 3-15.
- Isaev, N.V., V.M. Sorokin, V.M. Chmyrev, O.N. Serebryakova and O.Ya. Ovcharenko (2002). Electric fields in ionosphere connected with sea storms and typhoons, *Geomagn. Aeronomy*, 42, 670-675.
- Kim, V.P. and V.V. Hegai (1999). A possible presage of strong earthquakes in the night-time mid-latitude F2 region ionosphere, in *Atmospheric and Ionospheric Electromagnetic Phenomena Associated with Earthquakes* M. Hayakawa (Editor), Terrapub, Tokyo, 619-627.
- King, C.-Y. (1986). Gas geochemistry applied to earthquake prediction: an overview, *J. Geophys. Res.*, 91(B12), 12269-12281.
- Klimenko, M.V., V.V. Klimenko, I.E. Zakharenkova, S.A. Pulinets, B. Zhao and M.N. Tsidilina (2011). Formation mechanism of great positive TEC disturbances prior to Wenchuan earthquake on May 12, 2008, *Adv. Space Res.*, 48, 488-499.
- Klimenko, M.V., V.V. Klimenko, I.E. Zakharenkova and S.A. Pulinets (2012). Variations of equatorial electrojet as possible seismo-ionospheric precursor at the occurrence of TEC anomalies before strong earthquake, *Adv. Space Res.*, 49, 509-517.
- Liu, J.Y., H.F. Tsai and T.K. Jung (1996). Total electron content obtained by using the global positioning system, *Terr. Atmos. Ocean. Sci.*, 7, 107-117.
- Liu, J.Y., Y.J. Chuo, S.J. Shan, Y.B. Tsai, Y.I. Chen, S.A. Pulinets and S.B. Yu (2004). Pre-earthquake ionospheric anomalies registered by continuous GPS TEC measurements, *Ann. Geophys.*, 22, 1585-1593.

## A model of TEC perturbations possibly related to seismic activity

- Lyon, G.L. (1972) Geothermal Gases, in Natural gases in marine sediment I.R. Kaplan (Editor), Plenum press, New York and London, 141-150.
- McCartney, B.S. and B.M. Bary (1965). Echo-sounding on probable gas bubbles from bottom of Saanish Inlet, British Columbia, *Deep-Sea Res.*, 12, 285-293.
- Molchanov, O., E. Fedorov, A. Schekotov, E. Gordeev, V. Chebrov, V. Surkov, A. Rozhnoi, S. Andreevsky, D. Iudin, S. Yunga, A. Lutikov, M. Hayakawa and P.F. Biagi (2004). Lithosphere-atmosphere-ionosphere coupling as governing mechanism for preseismic short-term events in atmosphere and ionosphere, *Nat. Hazard. Earth Sys.*, 4, 757-767.
- Namgaladze, A.A., M.V. Klimenko, V.V. Klimenko and I.E. Zakharenkova (2009). Physical mechanism and mathematical modeling of earthquake ionospheric precursors registered in total electron content, *Geomagn. Aeronomy*, 49, 252-262.
- Okada, Y., S. Mukai and R.P. Singh (2004). Changes in atmospheric aerosol parameters after Gujarat earthquake of January 26, 2001, *Adv. Space Res.*, 33, 254-258.
- Omori, Y., Y. Yasuoka, H. Nagahama, Y. Kawada, T. Ishikawa, S. Tokonami and M. Shinagi (2007). Anomalous radon emanation linked to preseismic electromagnetic phenomena. *Nat. Hazard. Earth Sys.*, 7, 629-635.
- Omori, Y., Y. Nagahama, Y. Kawada, Y. Yasuoka, T. Ishikawa, S. Tokonami and M. Shinogi (2008). Preseismic alteration of atmospheric electrical conditions due to anomalous radon emanation, *Phys. Chem. Earth*, 33, 276-284.
- Pulinets, S.A., V.A. Alekseev, A.D. Legenka and V.V. Khagai (1997). Radon and metallic aerosols emanation before strong earthquakes and their role in atmosphere and ionosphere modification, *Adv. Space Res.*, 20, 2173-2176.
- Pulinets, S.A., K.A. Boyarchuk, V.V. Hegai, V.P. Kim and A.M. Lomonosov (2000). Quasi-electrostatic model of atmosphere-thermosphere-ionosphere coupling, *Adv. Space Res.*, 26, 1209-1218.
- Pulinets, S.A. (2009). Physical mechanism of the vertical electric field generation over active tectonic faults, *Adv. Space Res.*, 44, 767-773.
- Qin, K., L.X. Wu, S. Zheng, Y. Bai and X. Ly (2014). Is there an abnormal enhancement of atmospheric aerosol before the 2008, Wenchuan earthquake? *Adv. Space Res.*, 54, 1029-1034.
- Rulenko, O.P. (2000). Operative precursors of earthquakes in the near-ground atmosphere electricity, *J. Volcanol. Seismol.*, 4, 57-68.
- Ruzhin, Y.Y., V.M. Sorokin and A.K. Yashchenko (2014). Physical Mechanism of Ionospheric Total Electron Content Perturbations over a Seismoactive Region, *Geomagnetism and Aeronomy*, 54, 337-346.
- Smirnov, S. (2020). Negative Anomalies of the Earth's Electric Field as Earthquake Precursors, *Geosciences*, 10(1):10.
- Sorokin, V.M. and V.M. Chmyrev (1999). Modification of the ionosphere by seismic related electric field, in *Atmospheric and Ionospheric Electromagnetic Phenomena Associated with Earthquakes*, Hayakawa, M., Ed., Tokyo: Terra Sci., 805-818.
- Sorokin, V.M., N.V. Isaev, A.K. Yaschenko, V.M. Chmyrev and M. Hayakawa (2005a). Strong DC electric field formation in the low latitude ionosphere over typhoons, *J. Atmos. Sol.-Ter. Phys.*, 67, 1269-1279.
- Sorokin, V.M., A.K. Yaschenko, V.M. Chmyrev and M. Hayakawa (2005b). DC electric field amplification in the mid-latitude ionosphere over seismically active faults, *Natural Hazards and Earth System Sciences.*, 5, 661-666.
- Sorokin, V.M., A.K. Yaschenko and M. Hayakawa (2006). Formation mechanism of the lower-ionospheric disturbances by the atmosphere electric current over a seismic region, *Journal of Atmospheric and Solar-Terrestrial Physics*, 68, 1260-1268.
- Sorokin, V.M., A.K. Yaschenko and M. Hayakawa (2007). A perturbation of DC electric field caused by light ion adhesion to aerosols during the growth in seismic-related atmospheric radioactivity, *Nat. Haz. Earth Syst. Sci.*, 7, 155-163.
- Sorokin, V.M. and M. Hayakawa (2013). Generation of seismic-related DC electric fields and lithosphere-atmosphere-ionosphere coupling, *Modern App. Sci.*, 7, 1-25.
- Sorokin, V.M. and M. Hayakawa (2014). Plasma and electromagnetic effects caused by the seismic-related disturbances of electric current in the global circuit. *Modern App. Sci.*, 8, 61-83.
- Sorokin, V.M., V.M. Chmyrev and M. Hayakawa (2015). *Electrodynamic Coupling of Lithosphere-Atmosphere-Ionosphere of the Earth*, Nova Science Publishers, New York, 355.
- Sorokin, V.M., V.M. Chmyrev and M. Hayakawa (2020). A Review on Electrodynamic Influence of Atmospheric Processes to the Ionosphere, *Open Journal of Earthquake Research*, 9, 113-141.
- Surkov, V.V. (2015). Pre-seismic variations of atmospheric radon activity as a possible reason for abnormal atmospheric effects, *Ann Geophys.*, 58, 5, A0554.

- Vershinin, E.F., A.V. Buzevich, K. Yumoto, K. Saita and Y. Tanaka (1999). Correlations of seismic activity with electromagnetic emissions and variations in Kamchatka region. in *Atmospheric and Ionospheric Electromagnetic Phenomena Associated with Earthquakes* M. Hayakawa (Editor), Terrapub, Tokyo, 513-517.
- Virk, H.S. and B. Singh (1994). Radon recording of Uttarkashi earthquake, *Geoph. Res. Lett.*, 21, 737-740.
- Voitov, G.I. and I.P. Dobrovolsky (1994). Chemical and isotope-carbon instabilities of natural gas flows in seismically active regions, *Izv. AN SSSR Fiz. Zem.*, 3, 20-31. (in Russian).
- Yasuoka, Y., G. Igarashi, T. Ishikawa, S. Tokonami and M. Shinogi (2006). Evidence of precursor phenomena in the Kobe earthquake obtained from atmospheric radon concentration, *Appl. Geochem.*, 21, 1064-1072.
- Zakharenkova I.E., I.I. Shagimuratov, N.Yu. Tepenitzina and A. Krankowski (2008). Anomalous Modification of the Ionospheric Total Electron Content Prior to the 26 September 2005 Peru Earthquake, *J. Atmos. Sol.-Ter. Phys.*, 70, 1919-1928.
- Zhang, X., H. Chen, J. Liu, X. Shen, Y. Miao, X. Duc and J. Qian (2012). Ground-based and satellite DC-ULF electric field anomalies around Wenchuan M8.0 earthquake, *Adv. Space Res.*, 50, 85-95.
- Zhang, X., X. Shen, S. Zhao, Lu Yao, X. Ouyang and J. Qian (2014). The characteristics of quasistatic electric field perturbations observed by DEMETER satellite before large earthquakes, *J. Asian Earth Sci.*, 79, 42-52.
- Zhao B., M. Wang, T. Yu, W. Wan, J. Lei, L. Liu and G. Xu (2010). Ionospheric total electron content variations prior to 2008 Wenchuan Earthquake, *Int. J. Remote Sensing*, 31, 3545-3557. <https://doi.org/10.1080/01431161003727622>
- Zolotov O.V., A.A. Namgaladze, I.E. Zakharenkova, I.I. Shagimuratov and O.V. Martynenko (2008). Simulations of the equatorial ionosphere to the seismic electric field sources, in *Proceedings of the 7th International Conference "Problems of Geocosmos"*, St. Petersburg, Russia, 26-30 May, 2008, 492-496.

**\*CORRESPONDING AUTHOR: Victor M. NOVIKOV,**

Joint Institute for High Temperatures, Russian Academy of Sciences, Moscow, Russia  
and Sadovsky Institute of Geosphere Dynamics, Russian Academy of Sciences, Moscow, Russia  
e-mail: novikov@ihed.ras.ru